Supporting information:

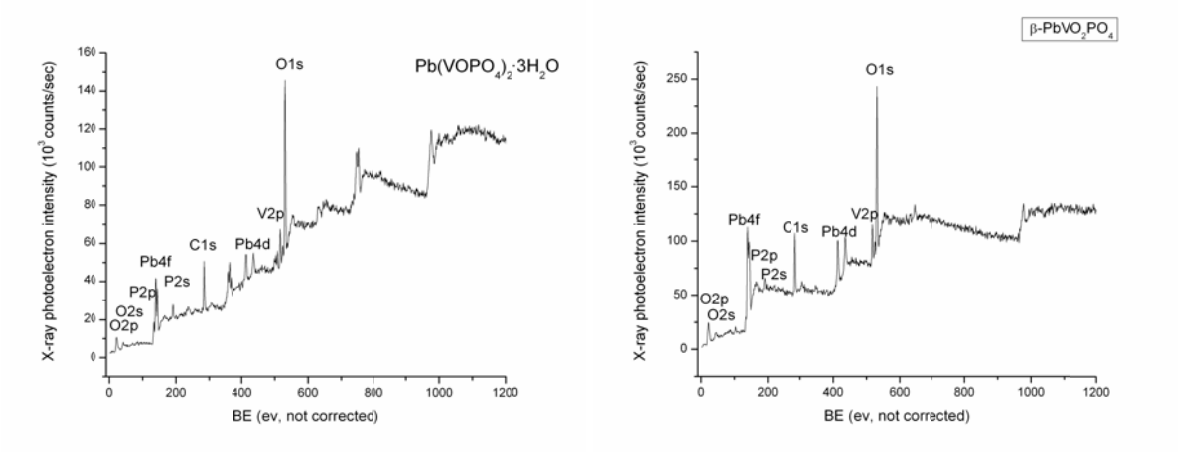

A B

Figure S1. The wide scan spectrums of XPS for $Pb(VOPO_4)_2{\cdot}3H_2O$ (A) and β-$PbVO_2PO_4$ (B)

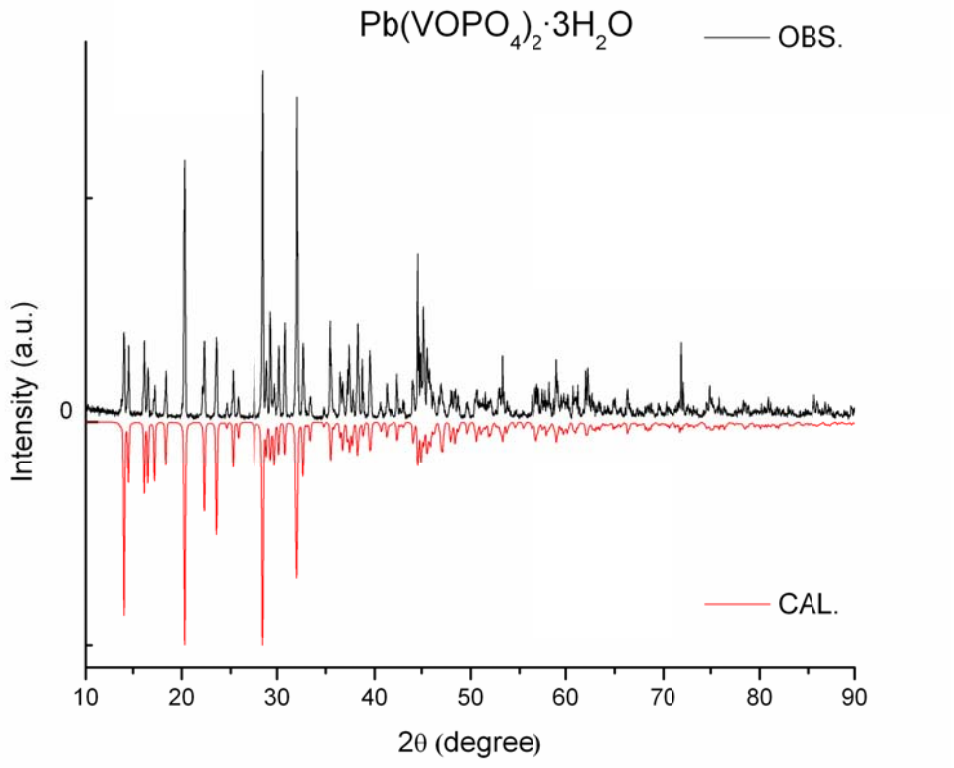

A

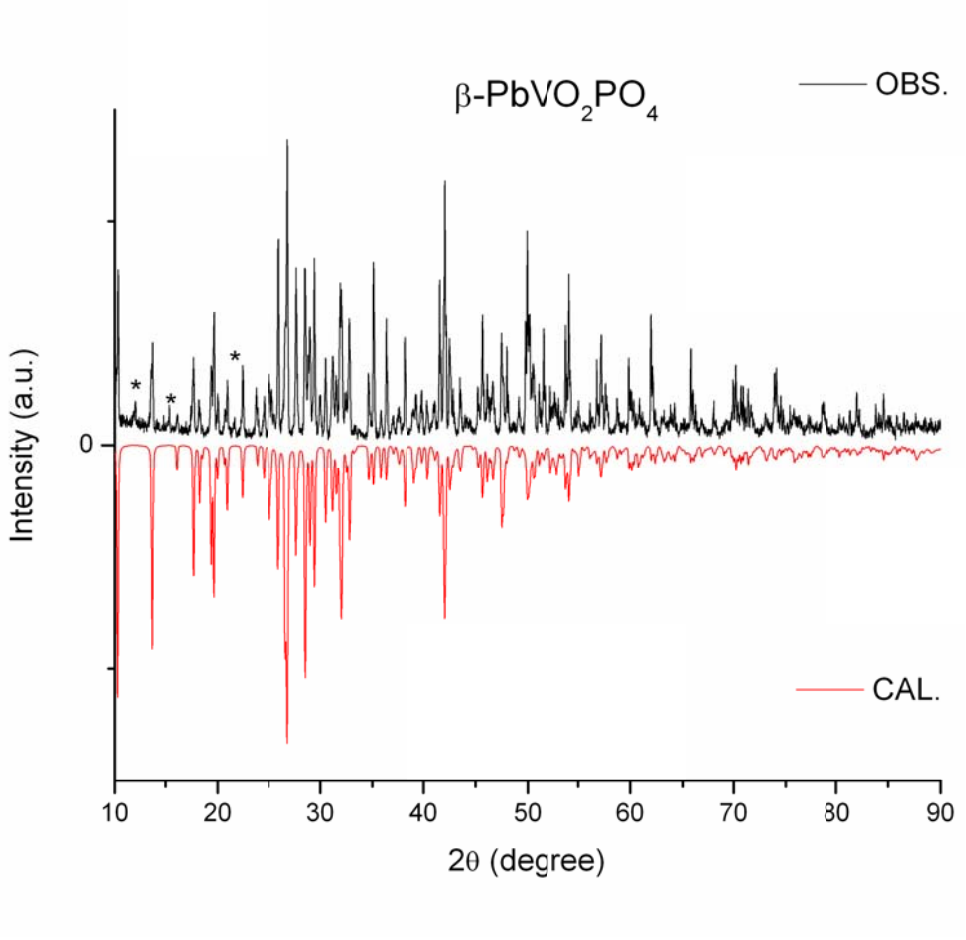

B

Figure S2. Powder XRD patterns for $Pb(VOPO_4)_2{\cdot}3H_2O$ (A) and β-$PbVO_2PO_4$ (B). Small peaks from the impurity marked as was observed between 10-20 two theta of the powder XRD pattern for β-$PbVO_2PO_4$.

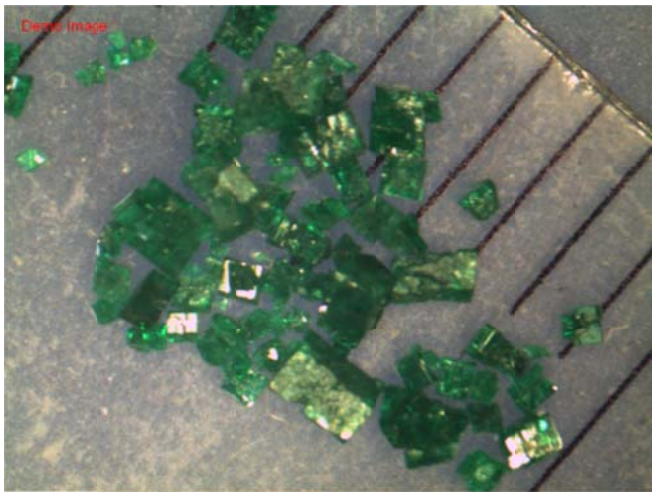

A

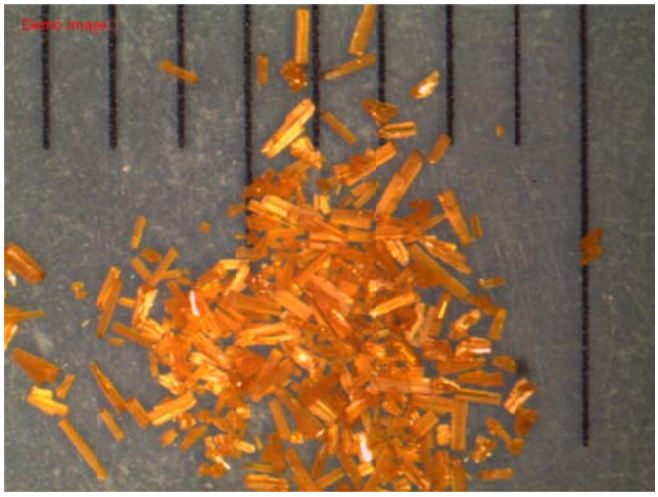

B

Figure S3. Microscope photos of $Pb(VOPO_4)_2 \cdot 3H_2O$ (A) and β-$PbVO_2PO_4$ (B) with the scale in mm.

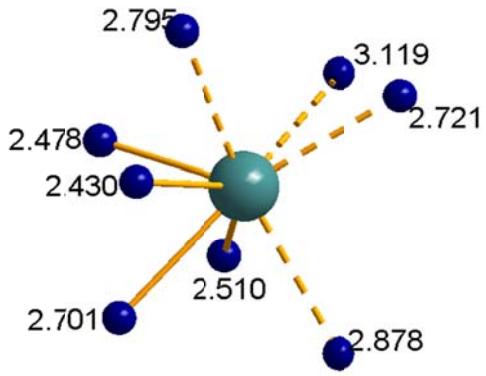

Figure S4. The coordination of oxygen atoms around Pb showing the stereoactivity of the lone pair.

Magnetic data part:

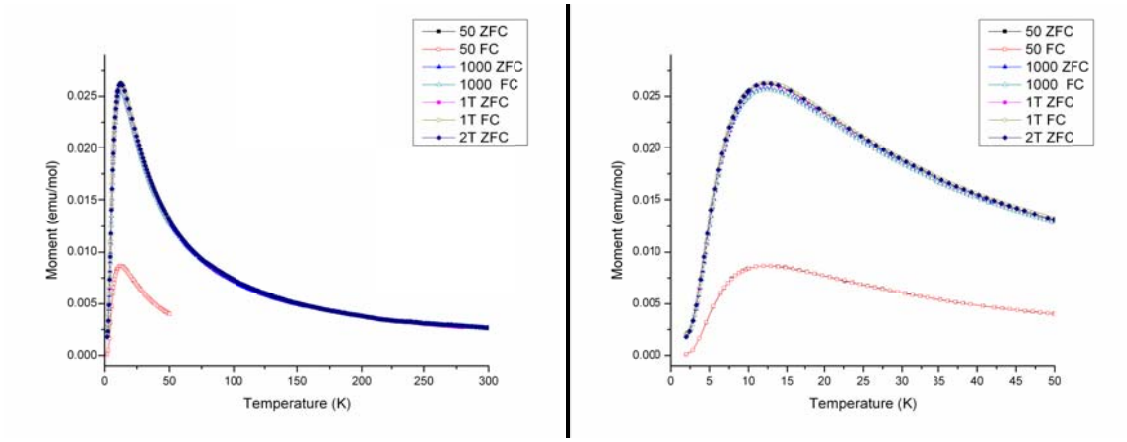

Figure S5. ZFC/FC curves recorded under different applied magnetic field.

The obvious difference between the ZFC/FC curves under 50 Oe with other ZFC/FC curves under higher field is due to the strong diamagnetic contribution (from the capsule and sample) at low field. The same reason for the slight lower of the ZFC/FC curves under 1000 Oe than curves under 1T and 2T. The Curves recorded at 1T and 2T was totally overlapped.

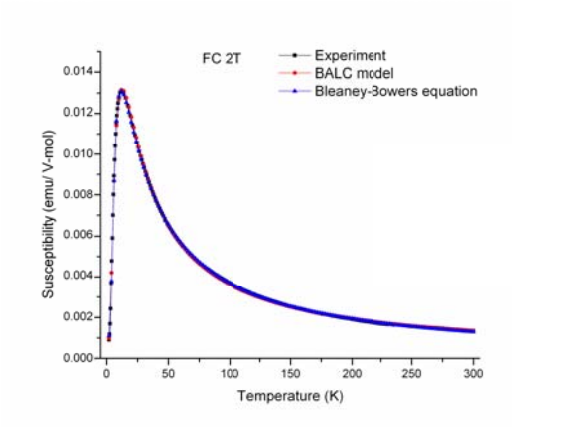

Figure S6. FC data recorded under the applied magnetic field 2T and was fit with BALC model and Bleaney-Bowers equation.

Use the FC data measured at 2T field with sweep mode. With BALC model, we were able to get a good fit yielding the alternating exchange coupling constant J_1= -6.63 cm^{-1}, α=0.49, g=2.00, χ_0= 9.34×10^{-5} emu/ V-mol， C_{imp}=0.007 emu K/ V-mol and Θ_{imp}=0.74 K with R^2=0.9998. Bleaney-Bowers equation provides a good fit yielding J= -6.95 cm^{-1}, g=2.06, and J'= -5.55 K, χ_0= -8.19×10^{-5} emu/V-mol， C_{imp}= 0.03 emu K/ V-mol and Θ_{imp}=-25.5 K with R^2=0.99974. Using equation (2) in the manuscript, the best refined n value was 1.38 and get the Δ=8.6cm^{-1} at final fitting with n=1.The results are consistent well with the fit using data measured under 5000 Oe with step mode.

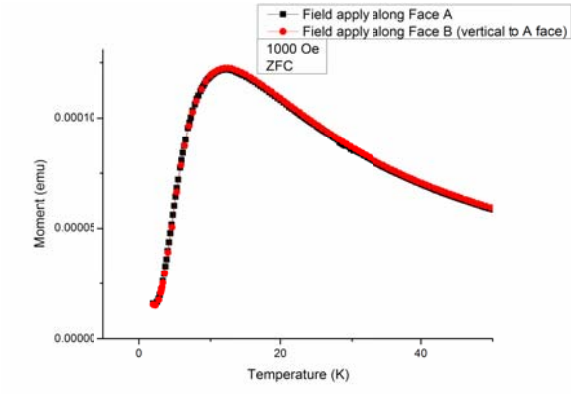

Figure S7. ZFC magnetic measurement (sweep model, 1K/min) applied on a single crystal along various direction A and B (B vertical to A). No mismatch was found, which implies the isotropic magnetic property.

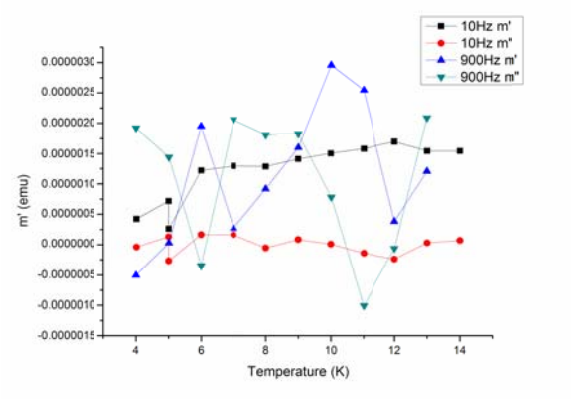

Figure S8. AC magnetic moment with 10Hz and 900Hz. The signal is weak with big noise. This measurement confirms the lack of long range order in the system.

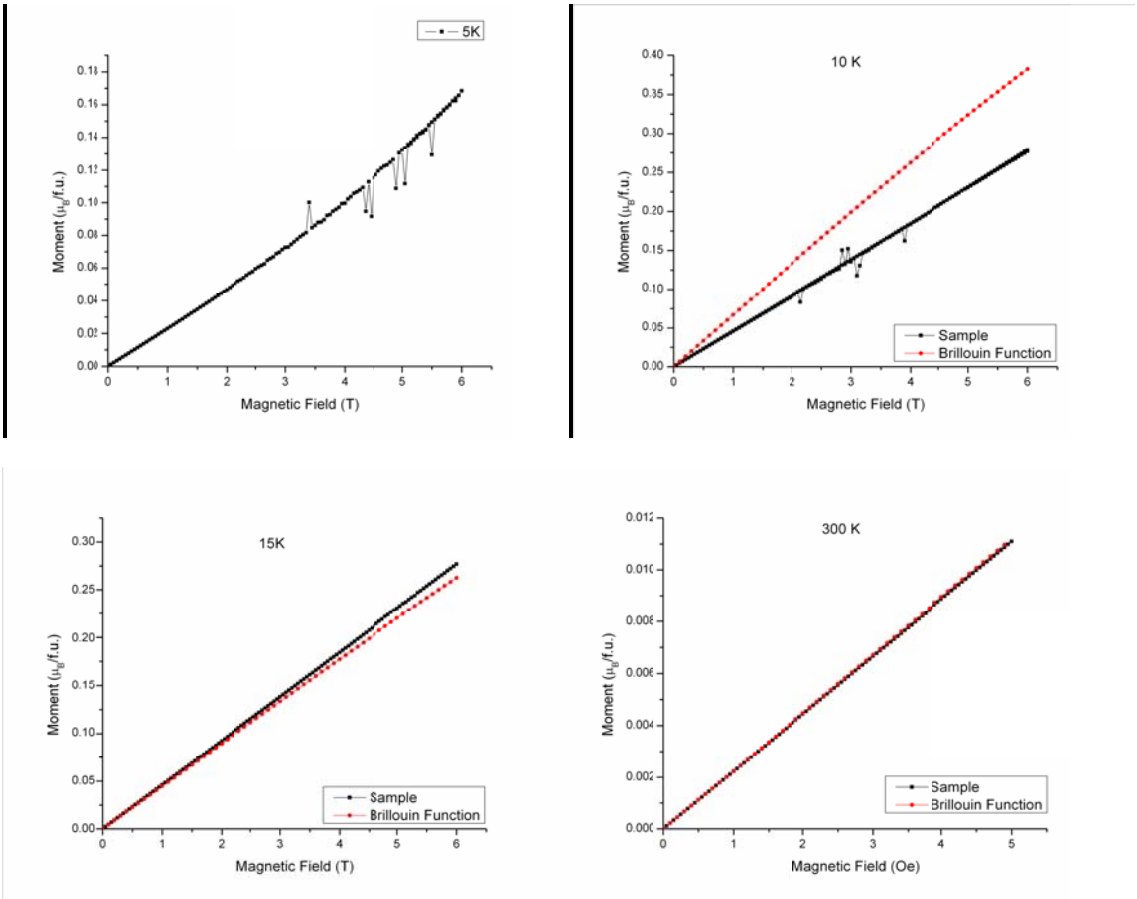

Figure S9. Isothermal magnetization measured between 0-6T applied field at 2K, 5K, 10K, 15K and 300K(0-5T).

Table S1. Exponents ζ_i and Valence Shell Ionization Potentials H_{ii} of Slater-Type Orbitals χ_i Used for Extended Hückel Tight-Binding Calculation[a]

atom	χ_i	H_{ii}(eV)	ζ_i	C^b	ζ_i'	C'^b
O	2s	-32.299999	2.275000	1.00000		
	2p	-14.800000	2.275000	1.00000		
V	4s	-8.810000	1.300000	1.00000		
	4p	-5.520000	1.300000	1.00000		
	3d	-11.000000	4.750000	0.475500	1.700000	0.705200
P	2s	-18.600000	1.750000	1.00000		
	2p	-14.000000	1.300000	1.00000		

[a] H_{ii}'s are the diagonal matrix elements $\langle \chi_i|H^{\text{eff}}|\chi_i \rangle$, where H^{eff} is the effective Hamiltonian. In our calculations of the off-diagonal matrix elements $H^{\text{eff}} = \langle \chi_i|H^{\text{eff}}|\chi_j \rangle$, the weighted formula was used. Contraction coefficients used in the double-ζ slater-type orbital.